STRUCTURAL AND MECHANICAL CHARACTERIZATION OF CALCIUM PHOSPHATE CEMENTS (CPCs) WITH DIFFERENT POWDER-LIQUID RATIOS

by

Şule Yetiş

B.S. in Biomedical Engineering, Erciyes University, 2014

Submitted to the Institute of Biomedical Engineering
in partial fulfillment of the requirements
for the degree of
Master of Science
in
Biomedical Engineering

Boğaziçi University
2019

ACKNOWLEDGMENTS

First of all, I would like to thank to my thesis advisor, Assist. Dr. Duygu EGE for her precious supervision and motivation during my research. I want to thank our laboratory members, Öznur Demir Oğuz and İlayda Duru for their precious guidance. I also would like to thank to my labmate Esra Güben for her friendship and all the fun we have had together. Our theory of the better will be always remembered.

I am grateful to my family for their encouragement and support throughout my thesis process. I would never have been able to achieve my thesis without their contribution. Lastly, I thank to Mehmet Ali Arıcı for his endless patience and love that is very precious for me.

ACADEMIC ETHICS AND INTEGRITY STATEMENT

I, Şule Yetiş, hereby certify that I am aware of the Academic Ethics and Integrity Policy issued by the Council of Higher Education (YÖK) and I fully acknowledge all the consequences due to its violation by plagiarism or any other way.

Name :

Signature:

Date:

ABSTRACT

STRUCTURAL AND MECHANICAL CHARACTERIZATION OF CALCIUM PHOSPHATE CEMENTS (CPCs) WITH DIFFERENT POWDER-LIQUID RATIOS

Calcium phosphate cements (CPCs) are encouraging osteoconductive bone substitutes for bone grafting. In this study, new bone cements were prepared by mixing powders of tetra calcium phosphate (TTCP), dicalcium phosphate dihydrate (DCPD) and calcium sulfate dehydrate (CSD) to polymeric solution including CMC and gelatin. Samples with different powder-to-liquid ratio (62.5, 65, 67.5, and 70%) were fabricated and characterized. Scanning Electron Microscopy (SEM), mechanical testing, Fourier Transform Infrared Spectroscopy (FTIR), Thermo-gravimetric Analysis (TGA), and X-ray diffraction (XRD) Analysis were performed to characterize mechanical and structural properties of synthesized composites. FTIR results confirmed the electrostatic interaction between COO^- groups in carboxymethyl cellulose (CMC) and Ca^{2+} ions released from CPCs. Hydroxyapatite (HA) formation was observed and assessed via XRD and SEM analysis on the samples incubated in phosphate buffer saline (PBS) solution for 28 days. Furthermore, the compressive strength values of composites were calculated as 1.63 ± 0.046, 1.53 ± 0.053, 0.91 ± 0.015 and 1.28 ± 0.072 MPa for P62.5, P65, P67.5, and P70, respectively. The overall results show that composite with 65% powder ratio may be appropriate for applications in the field of bone tissue engineering considering that it has the most proper mixture of the powder and liquid phase, high HA formation and sufficient mechanical properties for bone regeneration.

Keywords: Calcium phosphate, carboxymethyl cellulose, composite, mechanic, bone.

ÖZET

FARKLI TOZ-SIVI ORANLI KALSİYUM FOSFAT ÇİMENTOLARININ YAPISAL VE MEKANİK KARAKTERİZASYONU

Kalsiyum fosfat çimentoları kemik grefti için umut veren osteokondüktif kemik ikameleridir. Bu çalışmada temel olarak karboksi metil selüloz ve jelatin içeren polimerik çözeltiye tetra kalsiyum fosfat (TTCP), dikalsiyum fosfat dihidrat (DCPD) ve kalsiyum sülfat dehidrat (CSD) tozlarının karıştırılmasıyla yeni kemik çimentoları hazırlanmıştır. Toz-sıvı oranı (62.5, 65, 67.5, and 70%) farklı olan örnekler üretilmiş ve karakterize edilmiştir. Sentezlenen kompozitlerin mekanik ve yapısal özelliklerini karakterize etmek için Taramalı Elektron Mikroskobu (SEM), mekanik testler, Fourier Dönüşümlü Kızılötesi Spectroskopisi (FTIR), Thermo-gravimetrik analiz, and X Işını Kırınımı (XRD) analizi gerçekleştirilmiştir. FTIR sonuçları CMC deki COO^{-} grupları ve CPCs' den salınan Ca^{2+} iyonları arasındaki elektrostatik etkileşimi doğrulamaktadır. Hidroksiapatit (HA) oluşumu XRD ve SEM analizleriyle 28 gün fosfat tamponlu tuz (PBS) çözeltisi içinde inkübe edilen örnekler üzerinde gözlemlendi ve değerlendirildi. Ayrıca kompozitlerin baskı dayanım değerleri sırasıyla P62.5, P65, P67.5 ve P70 için 1.63 ± 0.046, 1.53 ± 0.053, 0.91 ± 0.015 ve 1.28 ± 0.072 MPa olarak hesaplandı. Genel sonuçlar, en uygun toz-sıvı dağılımına, yüksek HA oluşumuna ve yeterli mekanik özelliklere sahip olması açısından; %65 toz oranına sahip kompozitlerin kemik doku mühendisliği için uygun olabileceğini göstermektedir.

Anahtar Sözcükler: Kalsiyum fosfat, karboksimetil selüloz, kompozit, mekanik, kemik, .

TABLE OF CONTENTS

LIST OF FIGURES

LIST OF TABLES

LIST OF SYMBOLS

COO^-	Carboxyl ion
Ca^{2+}	Calcium ion
PO_4^{3-}	Phosphate ion
OH^-	Hydroxide ion
CO_2	Carbon dioxide
P62.5	Composite with 62.5% powder ratio
P65	Composite with 65% powder ratio
P67.5	Composite with 67.5% powder ratio
P70	Composite with 70% powder ratio

LIST OF ABBREVIATIONS

DCPA	Dicalcium phosphate
TTCP	Tetra calcium phosphate
CPCs	Calcium phosphate cements
DCPD	Dicalcium phosphate dihydrate
CSD	Calcium sulfate dehydrate
SEM	Scanning Electron Microscopy
TGA	Thermo-gravimetric Analysis
FTIR	Fourier Transform Infrared Spectroscopy
XRD	X-ray diffraction
HA	Hydroxyapatite
PBS	Phosphate buffer saline
CMC	Carboxymethly cellulose
Gel	Gelatin
PLA	Poly(lactic acid
PMMA	poly(-methyl methacrylate)
CA	Citric acid
PLGA	Poly(lactic-co-gly-colic acid)
O	Oxygen
N	Nitrogen
P	Phosphate
C	Carbon
H	Hydrogen
MPa	Megapascal
GPa	Gigapascal
CNT	Carbon nanotube
GO	Grephene oxide

1. INTRODUCTION

1.1 Motivation

Bone fractures or defects due to osteoporosis, trauma and cancer have required the synthetic bone substitutes to repair them [1]. Although, autograft treatment is considered as gold standard for these diseases, bone substitutes are developed due to disadvantages in autografts such as limited accessibility and pain morbidity [2, 3].For bone repair and regeneration, various substitutive biomaterials are studied such as ceramics, polymers, metals, calcium phosphate, calcium carbonate, calcium sulphate, and bioactive glasses [4].

Over the past forty years, calcium phosphate cements (CPCs) have been become popular due to the ability of easy shapability and their biocompatibility in bone tissue engineering [3, 5]. In 1980s, it was found that the solubility of synthetic hydroxyapatite (HA) is low compared to that of CPCs including calcium phosphate salts such as dicalcium phosphate dehydrate (DCPD: $CaHPO_4.2H_2O$), tetra calcium phosphate [TTCP: $Ca_4(PO_4)_2O$], and dicalcium phosphate (DCPA: $CaHPO_4$) [4]. As well as its low solubility, synthetic HA particles used in bone substitutes are unstable leading to migration of the particles to surrounding tissue under action of the blood flow [6].

CPCs without additives have some challenges such as their slow degradation rate, low mechanical strength, brittleness, and disintegration in the case of direct experience of body fluids [7, 8, 9]. Recently, the incorporation of Ca-P to polymeric hydrogels have been studied to overcome mechanical and biological problems as well as improving cement cohesion [10, 11]. This approach which is known as dual setting provides the cement both mechanism of dissolution-precipitation and organization of Ca^{2+} - acid chelates by deprotonating the organic acid of the polymer, which results in increase of the strength and decrease in brittleness of the cement [11].

Carboxymethyl cellulose (CMC) is a soluble, biocompatible polysaccharide due to its hydroxyl group and bounded water molecules, which has also the ability to trigger osteogenic differentiation and advanced mechanical properties in physicochemical environments [12, 13]. Rathna et. al. indicated that to form the complex of polysaccharide-protein is an attempt to mimic biological tissue [14]. It was reported that gelatin is a highly potential polymer working with CMC in tissue engineering [2]. Gelatin (Gel), the main protein of bone tissue which is a derivative of collage, is widely used to produce polymeric hydrogel for tissue engineering [15, 16]. Sarkar et al. also attracted the attention to this phenomenon, using gelatin as a protein is morphologically same as the natural bone. Similarly, citric acid (CA) which naturally comprise of $\sim$1.6 % of the bone content is effective in the deposition or dissolution of bone apatite as calcium binding agent due to its multi-carboxylic structure [9, 17, 18].

Considering this similarity, many studies have reported that CPCs which are prepared by dispersing in the natural and synthetic polymeric solution, and led to practical results [19, 20, 21]. In this study, composites of CPCs with different wt% of the powder phase, which contain CMC, gelatin and CA in the liquid phase were evaluated and compared after their characterization. Overall, prepared composites might be potential candidates for bone substitution applications.

1.2 Objectives

This study aims to improve the novel CPCs-based hydrogel by varying powder-to-liquid ratio. Objectives are as follows:

- To identify optimum powder-to-liquid ratio
- To optimize processing of CPCs
- To investigate effects of different percentage of powder on hydrogel
- To characterize chemical structure of conjugation between CMC and calcium

phosphate

- To increase cohesion of the CPCs due to prepared polymeric hydrogel
- To facilitate tissue ingrowth for the future study by improving pore structure

1.3 Outline

This thesis is composed of 5 chapters, which are as follows: Introduction is presented in Chapter 1 which includes motivation, objectives, and outline of the study. Chapter 2 provides background about structure and mechanic of bone, bone grafting, and further information related materials which is used in preparation of composites in this study. Experimental procedures are explained in Chapter 3. In Chapter 4, results of study are given. Discussion which is based on results of characterization is present in Chapter 5. Lastly, Chapter 6 comprises of conclusion and future works.

2. BACKROUND

2.1 Structure of Bone

Bone tissue plays a crucial role in mechanical support in the body, which is chemically composed of organic, inorganic, and water components. Organic component is constituted of type 1 collagen (20-25% of bone), whereas inorganic component includes apatite mineralized with calcium and phosphate which is approximately responsible for 65% of bone and water responsible for 10% of bone [22].

Bone tissue, which is non-homogeneous, an-isotropic, and porous at the macrostructure level, constitutes of two different structures: cortical (compact) and cancellous (trabecular) bone. Cortical bone (outer side of bone) has 10vol% porosity, whereas cancellous bone (inner side of bone) has 50-90 vol% porosity [23]. Trabecular bone is surrounded with the cortical bone which is well known as sandwich-type structure in engineering, as shown in Figure 2.1

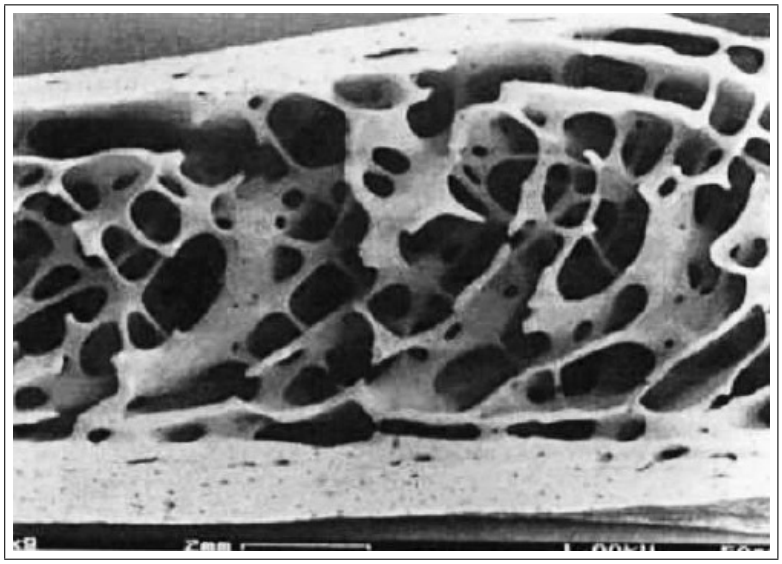

Figure 2.1 Structure of Cortical and Trabecular bone [24].

Compact bone constitutes 80% of total bone [25].The hierarchical structure of compact bone is organized from nanometer to macrometer, as shown in Figure 2.2 [26].

Collagen which is mineralized with carbonated apatite constitutes the basic structure of bone at the nanostructure level, and forming fibrils. Collagen fibrils are arranged into a bundle known as fiber. Then, micron level starts to occur through parallel fiber laying to each other, leading to formation of lamella. Following this structure, osteon occurs as a unit of compact bone [26].

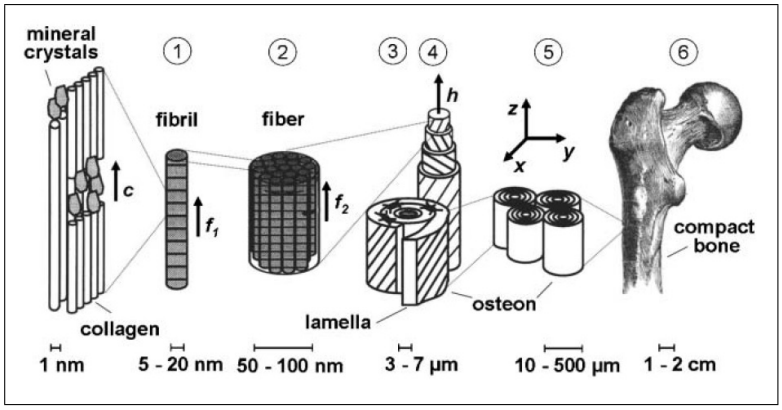

Figure 2.2 Hierarchical compact bone structure [26].

Cancellous bone which has 20% of total bone is less dense and lighter compared to compact bone [25]. In cancellous bone, lamellae are organized with the trabecular surface, described in Figure 2.3 [22] .

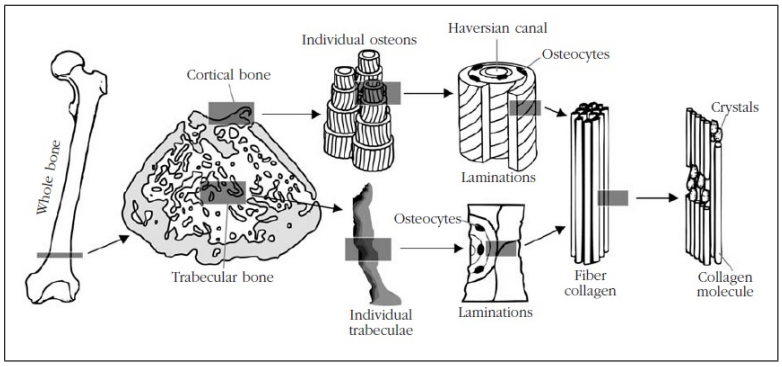

Figure 2.3 Cortical and cancellous bone structure [27].

2.2 Bone Mechanics

Mechanical behavior of bone has been balanced with changes of organic, inorganic, and water components [22]. These components provide the unique properties for bone [28]. Inorganic component provides the compression strength and stiffness whereas organic component is accounted for tensile properties [24].

Water as one of inorganic components also has great importance to support the mechanic of bone by carrying minerals. Decrease in water content refers to more mineralization in bone, resulting in more stiff and brittle structure which trigger easily breaking of bone. On the other hand, organic component in osseous tissue has also improved elasticity and ductility of bone [22].

Bone has the anisotropic structure which its properties change with respect to different reference directions. Degree of anisotropy can be defined by the orientations of trabeculae in cancellous bone tissue whereas by osteonal and lamellar orientation in the cortical bone. Stiffness and compressive resistance arise due to the arrangement of collagen fibers surrounded by crystal [24, 27]. According to this, cortical and cancellous bone tissues have different mechanical properties, as illustrated in Table 2.1.

Table 2.1
Biomechanical properties of different types of bone structures [25, 29].

Properties	Measurements	
	Cortical bone	Cancellous bone
Young's Modulus (GPa)	14-20	0.05-0.5
Compressive strength (MPa)	100-230	2-12
Tensile strength (MPa)	50-150	10-20
Density (g/cm^3)	18-22	0.1-1.0

To determine mechanical characteristics related to many biomaterials, and natural bone as well, stress-strain curves are utilized as shown in Figure 2.4, where are stress-strain curves of cortical and trabecular bone are comparatively illustrated.

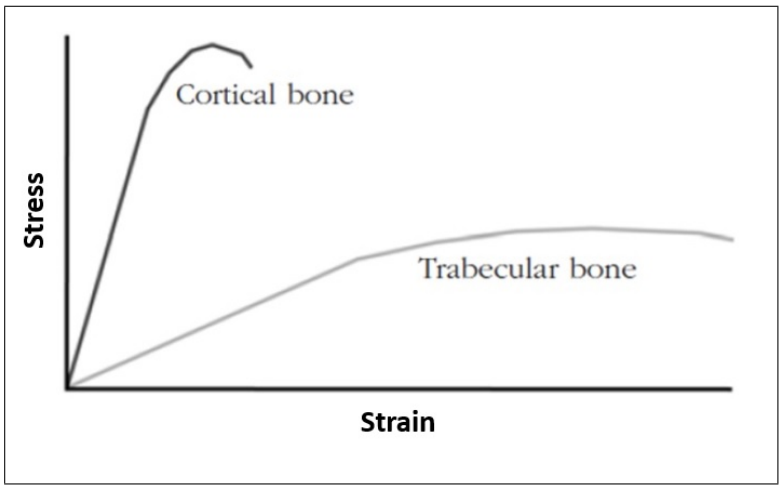

Figure 2.4 Stress-strain curves of various bone tissues [27].

There are some definitions to understand mechanical characteristics of bone tissue. Firstly, stress is generally known as the force per unit area in the literature. However, this value is in fact a local quantity, and for a tensile/compressive test, it is described as the average value of the force per cross section area because the stress is uniformly distributed. For different states of stress, it is defined a specific point of the material. They are different from each other. It should be noted that a (theoretically infinitesimally) small area should be considered to define the stress at a specific point. On the other hand, strain is defined as the displacement gradient at a material point, which can be thought as the ratio of overall deformation of material over the total length of material if the strain field is uniform such as an extended wire [30].

As shown in Figure 2.5, there are various loading types applied to bone tissue with different resulting stress states, which are named as compression, tension, shear, torsion, and bending. [31].

2.3 Bone grafting

Bone grafting is required to heal severe defects due to infection, trauma, tumor resection which cannot immediately restore its own tissue [32, 25]. It is a common

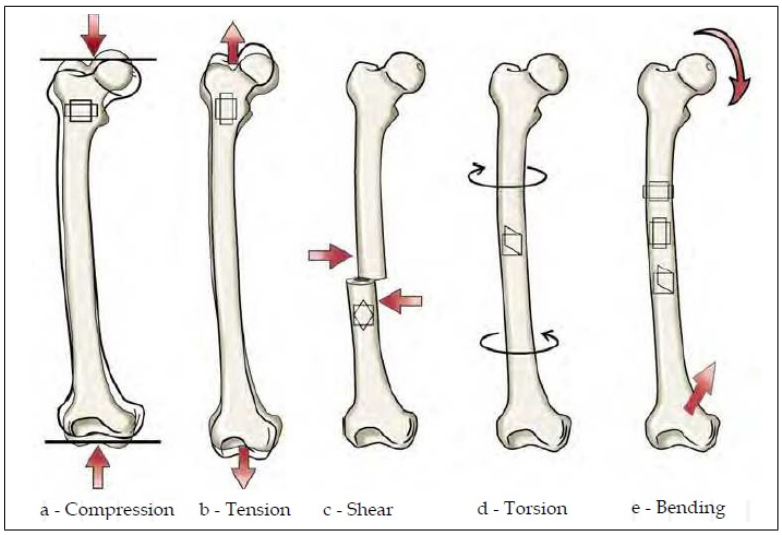

Figure 2.5 Various loads applied to bone [31].

surgical process to fill the defect and support the bone regeneration. There are three main bone grafting materials which are allografts, autografts, and synthetic bone graft [33]. There are many factors affecting the incorporation of grafted material in selecting bone graft material such as mechanical strength, biological response, pore size of material, and graft type [34].

Autografting is a technique which has the common usage in bone grafting due to its non-immunogenic, osteoinductive, and osteoconductive properties. It is performed as a tissue transplantation from one location to another location of the same human body. Although autograft is the most ideal bone grafting material because it has favorable properties of bone grafting materials such as osteoconduction, osteogenesis, osteoinduction, and osteointegration, it has some drawbacks such as short- or long-term pain, morbidity of donor site which occurs in around 20% of all patients [35]. Allograft is an another way of bone grafting to regenerate the bone tissue, which is bone transplant from one individual (donors or cadavers) to another one [25]. This alternative technique decreases donor-site morbidity of autografting. However, there are some challenges such as disease transmission, infection and limited availability for these techniques. Therefore, synthetic bone materials have become alternative approaches to overcome the limitations such as metal, polymer, and ceramic [3].

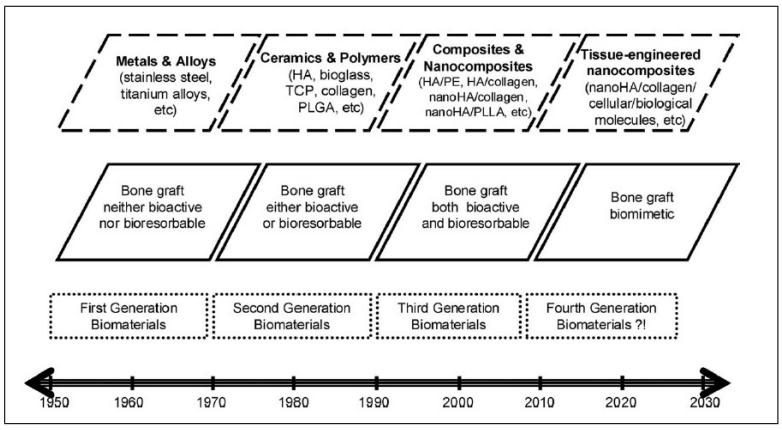

Figure 2.6 Development of synthetic bone grafting [25].

As illustrated in Figure 2.6, metallic biomaterials have been initially produced for orthopedics. Titanium alloys and stainless steel are the mostly used in load-bearing applications due to their strong and rigid structure. But limited osteointegration, inadequate bonding between metal implant and host tissue, and corrosion hinder the usage of metal implants in orthopedics. Moreover, although ceramics (bioglass, alumina, zirconia) are bioactive and bioinert materials for bone tissue applications, their drawbacks are considered as mechanical such as brittleness structure and poor tensile strength. Polymers (naturals: gelatin, chitosan,alginate; synthetics: poly(lactic-co-gly-colic acid)PLGA, poly(lactic acid)(PLA), poly(-methyl methacrylate)(PMMA)) are also insufficient to meet mechanical properties of bone. An ideal bone substitute has efficient mechanical properties and biocompatibility in the bone tissue engineering. Composites with polymer additives attract a great attention due to their biocompatibility, mechanical stability, and biodegradability [36].

2.4 Calcium Phosphate Cements

Calcium phosphate cements have been extensively used in bone substitute applications to repair bone defects due to the similar nature between calcium phosphate and mineral components of bone tissue [37]. They have attracted considerable attention thanks to their handling properties, high moldability, self-setting ability, and their biological performance in recent years [9, 32, 38].

Depending on their hydration setting reaction at different pH, there are basically two types of CPCs: hydroxyapatite ($Ca_{10}(PO_4)_6(OH)_2$, HA) and brushite ($CaHPO_4.2H_2O$, DCPD) or monetite ($CaHPO_4$, DCPA). CPCs tend to form the nanocrystalline hydroxyapatite (HA) at neutral or basic pH, whereas brushite or monetite are formed at pH<6 [10]. Setting time of brushite CPCs is shorter than that of apatite CPCs, which confirms that brushite CPCs are utilized as bone filling materials and apatite CPCs have potential as structural bone material [39].

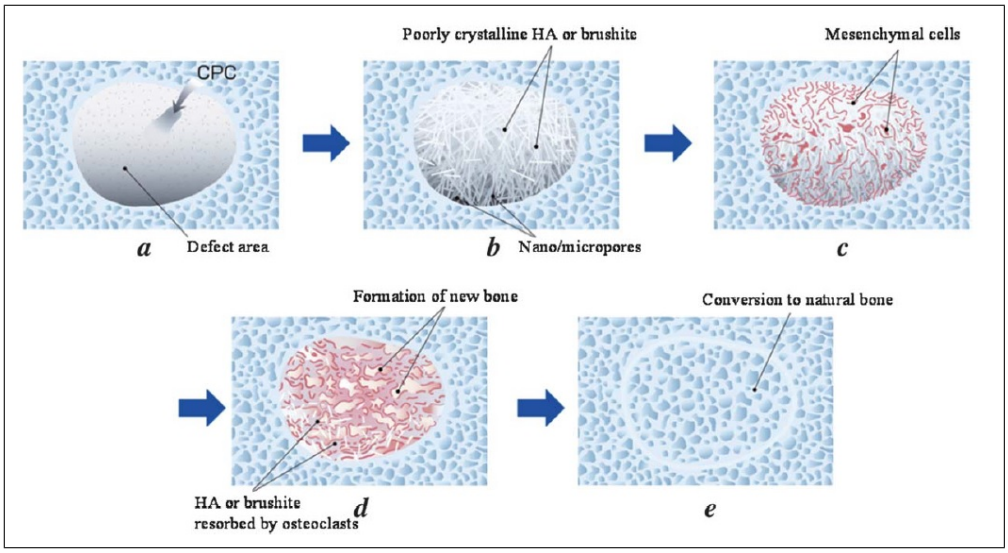

Figure 2.7 The process of bone regeneration with CPCs [39].

Binding between CPC grafted in bone defect area and bone tissue occurs when CPC is placed in bone defect area (Figure 2.7a). Then, CPC possessed porous structure provide fluid flow inside materials and this leads to HA formation (Figure 2.7b). Mesenchymal stem cells and growth factor are placed in cement surface and increase the bone tissue growth (Figure 2.7c). As a final level, the new natural bone forms by balancing degradation of CPC and formation of bone (Figure 2.7d and e) [39]. During this biological process, each level affects the bone substitutes in terms of mechanical or structural aspects. Thus, powder components of CPCs have a great importance on these physical properties.

CPCs consist solid and liquid phase, including powder of calcium phosphate compounds and aqueous solutions, respectively. In majority of studies, solid phase of CPCs compounds of tetra calcium phosphate (TTCP: $Ca_4(PO_4)_2O$), dicalcium phos-

phate dihydrate (DCPD) or dicalcium phosphate anhydrous (DCPA), and calcium sulphate dehydrate (CSD: $CaSO_4.2H_2O$) are used [40, 41, 42, 43]. HA formation from TTCP-DCPD reaction in solution, which has the ability of self-setting, is shown in Eq. 2.1.

$$2Ca_4(PO_4)_2O + 2CaHPO_4 = Ca_{10}(PO_4)_6(OH)_2 \text{ [40]} \tag{2.1}$$

Calcium sulfate dihydrate (CSD) has been used to fill void in bone defects in orthopedic applications since 1892. The property of its rapid resorption gives rise to create pores in incorporated material [44]. Occurred pores may allow the earlier osteogenic activity to promote healing process in bone, so it can balance the resorption of CSD and the rate of bone formation [45]. Moreover, addition of CSD accelerates setting time thanks to high amount of much calcium release. As shown in Eq. 2.2, dissolved CSD interact with phosphate ions to form HA crystals [46].

$$10CaSO_4.2H_2O + 6(HPO_4)^{2-} = Ca_{10}(PO_4)_6(OH)_2 + 8H^+ + 10(SO_4)^{2-} + 18H_2O \tag{2.2}$$

2.5 Polymeric Solution for CPCs

2.5.1 Carboxymethyl Cellulose (CMC)

CMC is a natural polymer which is obtained chemically modified natural derivative of cellulose [36]. It is commonly used in biomedical applications due to its hydrophilicity, nontoxicity, low cost, and biocompatibility [47]. As well as there is its extensive usage in drug delivery and wound dressing, many studies related to bone tissue engineering is included in the literature [48].

CMC has the ability of Ca^{2+} chelation through COO^- groups as well as carrying the sulfate in bone substitution owing to a large number of carboxyl and hydroxyl groups on its surface, as illustrated in Figure 2.8 [32, 49]. In this regard, CMC has ex-

cellent cohesion, stable mechanical properties and applicable biodegradability in CPCs [50].

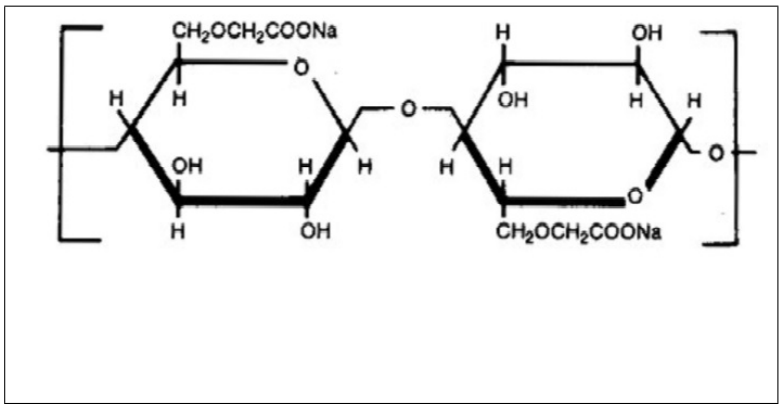

Figure 2.8 Sodium carboxymethyl structure.

2.5.2 Gelatin

Gelatin is a hydrolysis product which is a derivative natural protein from collagen [33, 51]. It has been extensively used in medicine pharmaceuticals, and food field. In tissue engineering, gelatin is benefited as crosslinked hydrogel which is necessary for stability and cell attachment [16]. For CPCs, there are studies which low concentration of gelatin enhances the mechanical properties of CPCs [15]. Furthermore, in terms of biological aspects, incorporating gelatin into CPCs improves the cell adhesion [3].

2.5.3 Citric Acid (CA)

CA is a weak organic acid containing one hydroxyl and three carboxyl groups, as shown in Figure 2.9.

It is naturally present in citrus fruits. In previous studies, it has been reported that bone and teeth contain $\sim \leq 20-80 \mu$mols/gram of citrate ions, which is comprising $\sim$1.6 % of the bone content [17, 52]. As well as its own carboxyl groups interact with between hydroxyl group of CMC as a crosslinker agent, it also impacts on the

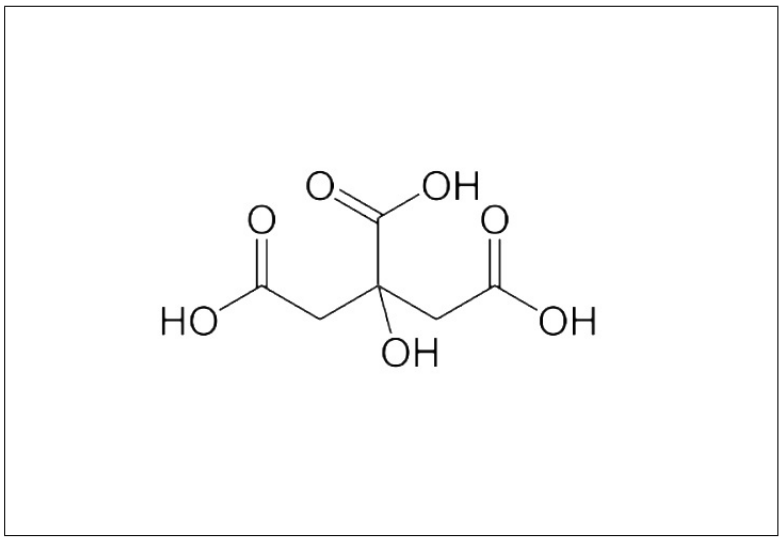

Figure 2.9 Chemical structure of citric acid.

accumulation and resolution of bone apatite as a calcium-binding agent [9, 18]. Also, it is suggested that TTCP treated with CA gives rise to HA formation and calcium citrate [53].

3. MATERIALS and METHODS

3.1 Synthesis of Hydrogel (Liquid Phase)

The liquid phase of composites mainly contains gelatin (Type B from bovine skin, gel strength ∼225 g Bloom), sodium carboxymethyl cellulose (NaCMC, Mw 250.000 kDa, ds 0.9), and sodium citrate tribasic dihydrate ($C_6H_5Na_3O_7$, Mw 294.10 g/mol, mp: >300°C (lit.). First, 10 wt% of gelatin solution was prepared by using 2.5 w/v% of Na_2HPO_4 (hardening agent) aqueous solution as a known accelerator dispersed in distilled water [54]. Gelatin solution was magnetically stirred for 15 min at 60 °C. Following the dissolution of gelatin, a total concentration of 2% by weight of Na_2HPO_4 solution, CMC powder was dissolved in gelatin solution by stirring for 45 min at 90 °C. After, the solution was reached to room temperature and continued stirring for 30 min by adding 20 wt% citric acid. To remove the excess water from hydrogel, final mixture was left at 30 °C in the oven for 24h, following more 24 h kept at 80 °C for esterification reaction [55, 56].

3.2 Preparation of Ca-P powder (Solid phase)

3.2.1 TTCP Synthesis

TTCP was prepared as powder mixture containing monetite (DCPA, $CaHPO_4$, Mw 136.06 g/mol, Sigma Aldrich (Taufkirchen, Germany)) and calcium carbonate ($CaCO_3$, $\leq 30\mu$m particle size, Mw 100.09 g/mol, d: 2.93 g, Sigma Aldrich (Taufkirchen, Germany)) in equimolar ratio according to Eq. 3.1, which was sintered at 1500 °C for 6h in the furnace (Thermo Fisher- K114) [6, 57].

$$2CaHPO_4 + 2CaCO_3 = Ca_4(PO_4)_2O + 2CO_2 + 3H_2O \tag{3.1}$$

The reaction was occurred by heating at a speed of 10 °C/min, followed cooling process by 10 °C/min. Then, sintered piece of TTCP was crushed by pestle and milled in agate jars until powder of 75 μm particle size is obtained.

3.2.2 Preparation of total solid phase

For the final powder mixture, in addition to TTCP, calcium hydrogen phosphate dihydrate (DCPD, $CaHPO_4.2H_2O$, d:2.31 g/mL, Mw 172.09 g/mol) from Sigma Aldrich (Taufkirchen, Germany) and calcium sulphate dihydrate (CSD, $CaSO_4.2H_2O$, Mw 172.17 g/mol) from Merck (Merck KGaA, Darmstadt, Germany) were used. Final CPC powder has consisted of TTCP, DCPD, and CSD. As in shown Table 3.1, TTCP and DCPD were mixed at the ratio of 76.65% and 23.35%, respectively, and then CSD formed 20% of total powder mixture [6, 58].

Table 3.1
The weight proportion of TTCP-DCPD and final CPC powder.

Powder mixture	***TTCP***	***DCPD***	***CSD***
TTCP-DCPD wt%	76.65	23.35	-
TTCP-DCPD-CSD wt% *(Final CPC powder)*	80		20

3.3 Preparation of hydrogel-CaP composites

Cement composites were prepared as labeled P62.5, P65, P67.5, and P70 according to their different liquid-to-powder ratio shown in Table 3.2. The solid phase and liquid phase were manually mixed until homogenous cement mixture was obtained. Then, cement paste was packed in syringes (without tips) with 10 mm diameter. The dimension ratio of composites was determined as 2:1(length-to-diameter). After setting procedure of composites which is treatment at 50 °C for 72h in an oven [59], they were immersed in PBS solution to trigger HA crystallization up to 28 days.

Table 3.2
The content percentage of composites with different powder-to-liquid ratio.

Samples	***Liquid Phase (wt%)***	***Solid Phase (wt%)***
	Liquid	*Powder*
	(2 w/v% CMC, 10 w/v% Gel, 20 w/v% CA)	*(TTCP-DCPD-CSD)*
P62.5	37.5	62.5
P65	35	65
P67.5	32.5	67.5
P70	30	70

3.4 Characterization of Composites

3.4.1 Fourier Transform Infrared (FTIR) Spectroscopy Analysis

FTIR spectroscopy (Thermo Scientific Nicolet 380 FT-IR spectrometer) was employed to estimate chemical interactions between CMC and CaP. The spectrum of samples was recorded in the range of 4000-400 cm^{-1}. FTIR analysis was performed at Boğaziçi University Chemistry Department.

3.4.2 Scanning Electron Microscopy (SEM) Analysis

Surface morphology and HA formation of composite samples were studied via scanning electron microscopy (Philips XL30) at Boğaziçi University. The incubated samples in PBS until 28 days were dried by using freeze-drying method, and coated with gold-palladium before SEM analysis.

3.4.3 X-Ray Diffraction (XRD) Analysis

X-ray diffraction (XRD; D/MAX-Ultima+/PC, Rigaku) analysis was used to characterize HA crystallization at Boğaziçi University Research and Development Cen-

ter. After incubation process of composites for 0 and 28 days, XRD analysis was performed between 10° and 40° at 40 kV and 30 mA with a step size of 0.02° .

3.4.4 Thermo-gravimetric Analysis (TGA)

Thermal stability of composites was evaluated using a thermogravimetric analysis (TGA; SII Nanotechnology-SII6000 Exstar TG/DTA 6300) between 30 °C and 1200 °C at a heating range of 10 °C min^{-1} under the nitrogen environment at Yıldız Technical University.

3.4.5 Mechanical Measurements

Composites were prepared with 10 mm diameter and 20 mm length for the mechanical analysis. For each group, five samples (n=5) were tested. After their incubation at 50°C for 72h, compressive strength and compressive modulus were measured with a crosshead displacement rate of 1 mm/min by using MTS 858 Mini Bionix II Universal Test Machine (Model number: 359.01, Part Number: 100-146-714, Rev: A, Serial Number: 10189576, load cell: 300 kg) adapted to system from ESIT (Elektronik Sistemler İmalat ve Ticaret), in Laboratory of Biomechanics and Strength of Materials, Faculty of Mechanical Engineering, Istanbul Technical University.

The strains on the samples were also determined by an optical 3D Correlation System (2 off 2.0 mp cameras and special lens, used with Vic3D Software, Correlated Solutions), shown in Figure 3.1. By using spray paint, the random speckle patterns were generated for image correlation on the cleaned sample surface, which is illustrated in Figure 3.2.

The load data and the optical strain measurements were combined to obtain the stress-strain curves of the samples. MATLAB and Microsoft Excel were used to process data which determine the compressive modulus of elasticity and compressive

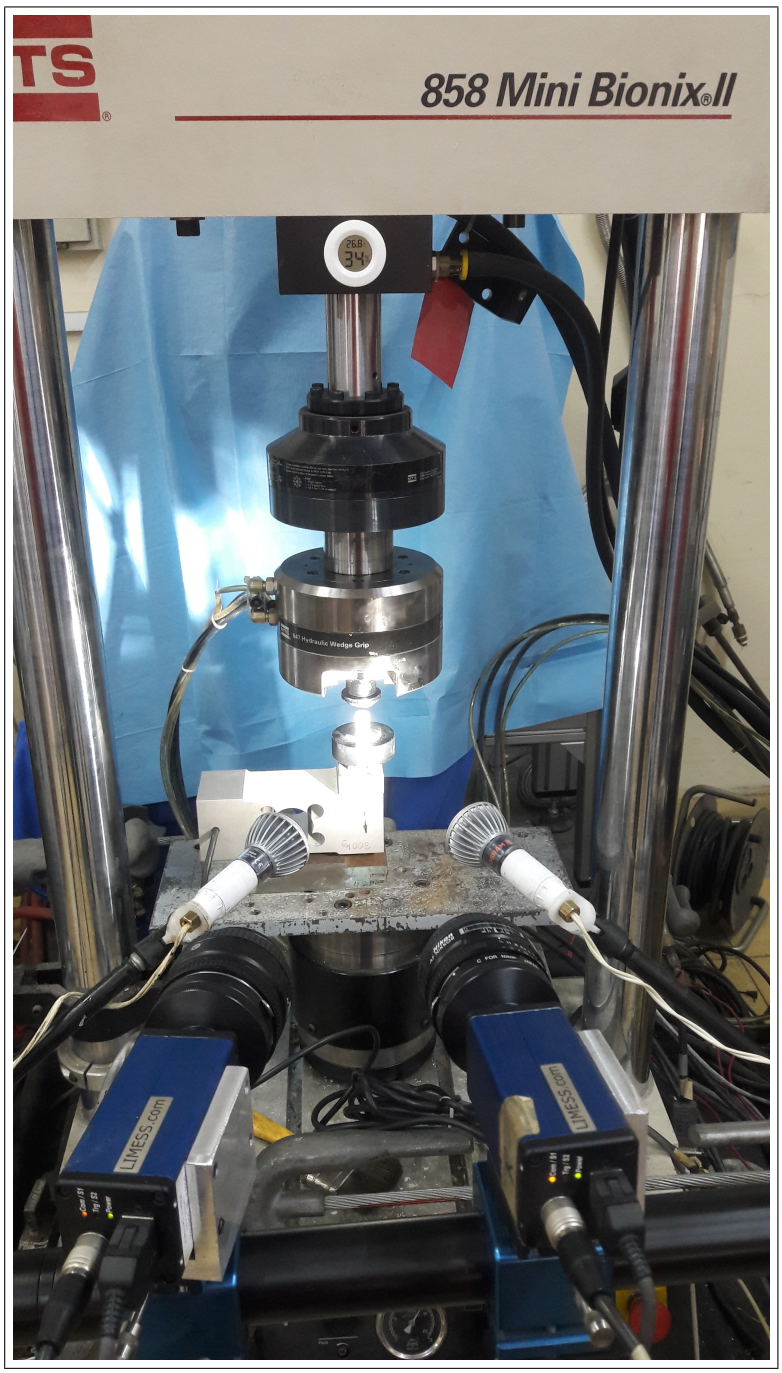

Figure 3.1 Experimental setup for mechanical testing.

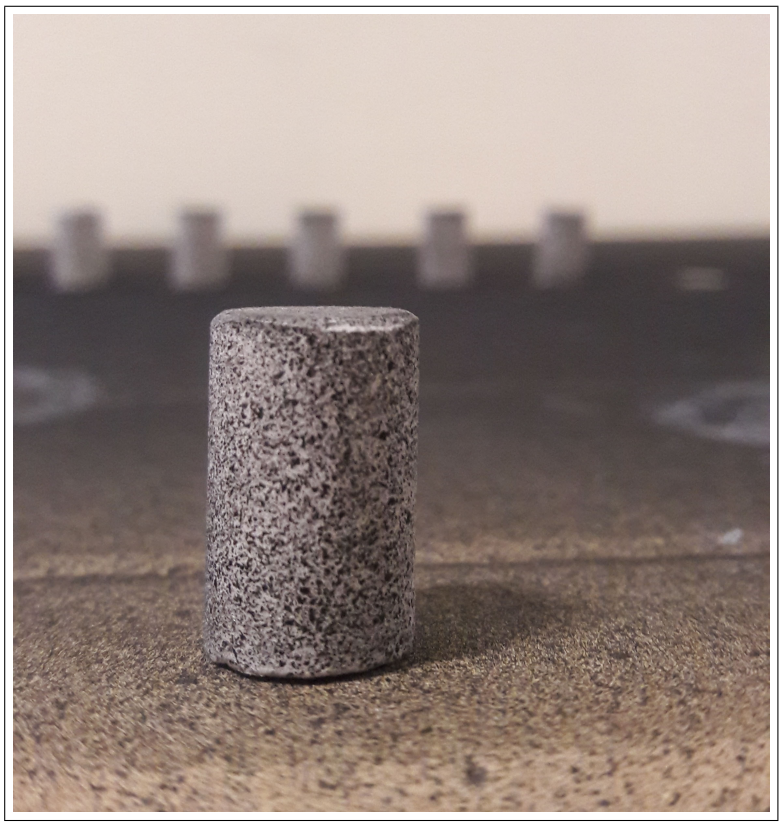

Figure 3.2 Sample with random speckles.

strength (i.e. failure stress) values.

3.5 Statistical Analysis

The statistical evaluation of results was performed applying one-way ANOVA analysis with Tukey's post-test via SPSS for Windows software.($p \leq 0.05$) was considered to be statistically significant.

4. RESULTS

4.1 Fourier Transform Infrared (FTIR) Spectroscopy Analysis

FTIR spectrum of the P65 composite and hydrogel were presented in Figure 4.1.

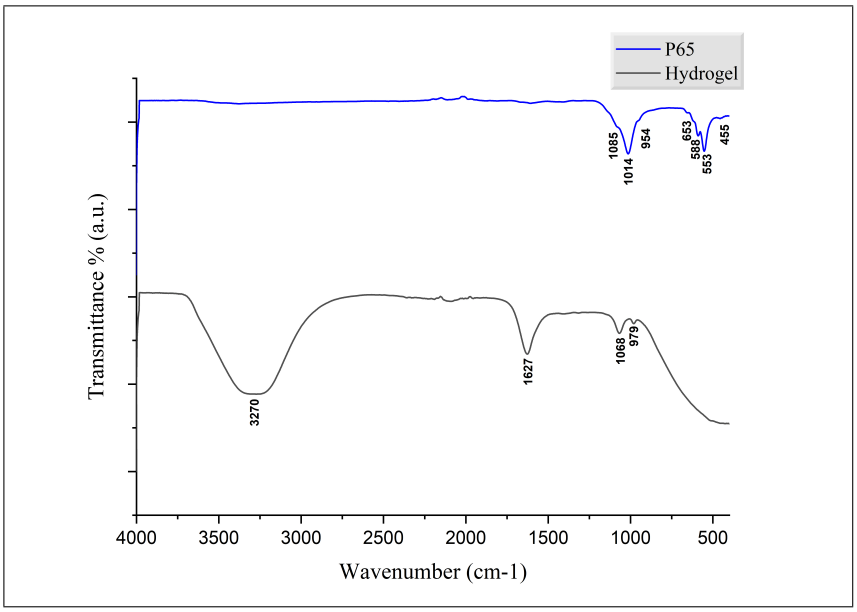

Figure 4.1 FTIR spectrum of liquid phase and final composite P65.

For the liquid phase of composite (hydrogel), FTIR spectrum of characteristic O-H stretching in CMC appeared at 3270 cm^{-1} band [51]. The spectra illustrated absorption bands between 1600-800 cm^{-1} which corresponded to characteristic bands of glycosidic bonds in CMC, which confirmed by C-O-C vibrations observed in 1068 and 979 cm^{-1} bands [51, 60]. 1627 cm^{-1} band assigned to asymmetric vibration of COO^{-} from CMC and N-H bending vibration from Gel [36, 51, 60].

In the spectrum of hardened composite, symmetric($v1$) and antisymmetric($v3$) P-O stretching vibrations of PO_4^{3-} ion which are characteristic for HA were assigned to 1085, 1014 and 954 cm^{-1} bands [61]. Moreover, 653 and 588 cm^{-1} bands in spectrum represented the P-O-P and O-P-O bending ($v4$) vibration, respectively [36, 61]. There-

fore, all bands in spectrum confirmed the HA formation in composites incorporated with the polymeric hydrogel.

4.2 Scanning Electron Microscopy (SEM) Analysis

SEM images of the four composites at day 0 and after incubation in PBS for 28 days are shown in Figure 4.2.

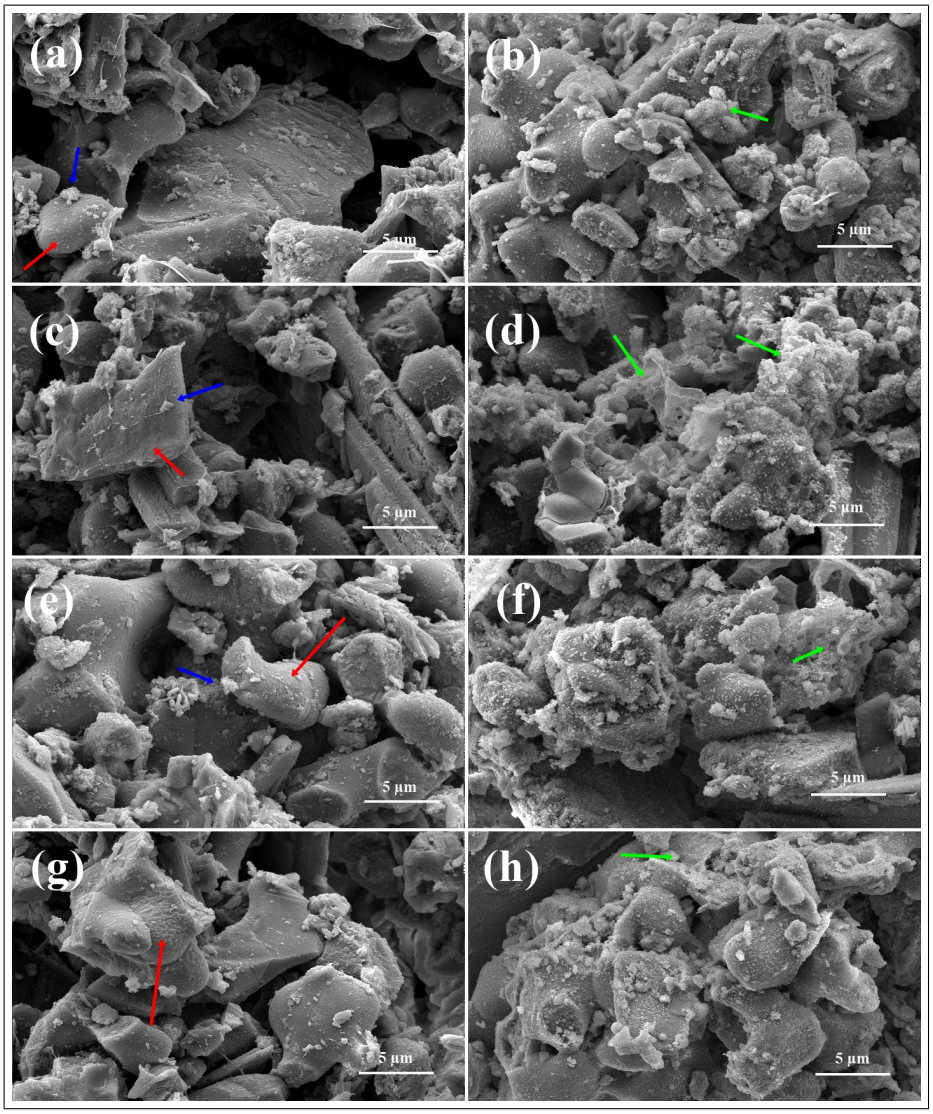

Figure 4.2 SEM images of P62.5 at day 0 (a) and day 28 (b), P65 at day 0 (c) and day 28 (d), P67.5 at day 0 (e) and day 28 (f), and P70 at day 0 (g) and day 28 (h). Red arrow (TTCP), blue arrow (DCPD) and green arrow (HA) showed specific structure.

SEM studies were carried to observe the accumulated of HA layer from TTCP-

DCPD-CSD on the surfaces of the cement samples. It can be seen that TTCP particles have round edges and smooth surfaces resulting in their sintering treatment, while DCPD particles are observed in irregular shape [62]. Formed apatite layer on the cement composites were in needle-like and flake-like apatite shape, shown with green arrow in Figure 4.2.

4.3 Mechanical Measurements

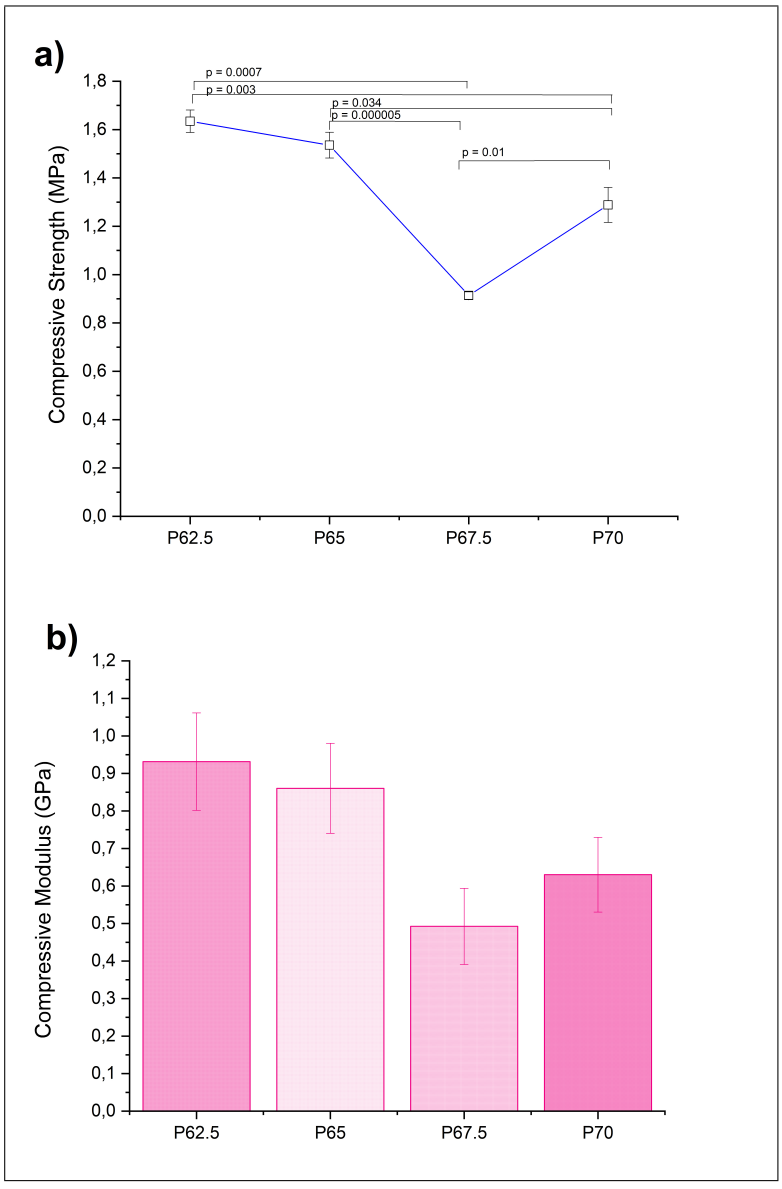

Figure 4.3 Compressive strength values (a) and compressive modulus (b) of composites.

Compressive modulus and compressive strength values of hardened composites were calculated via mechanical compression.Compressive strength values of composites (P62.5 and P65, 1.63 ± 0.046 and 1.53 ± 0.053 MPa, respectively) with low powder content were significantly higher than that of those (P67.5 and P70, 0.91 ± 0.015 and 1.28 ± 0.072 MPa, respectively) with high powder content ($p \leq 0.05$), as shown in Figure 4.3. Composite P70 had also significantly a higher compressive strength value than the composite P67.5 ($p \leq 0.01$). Significant difference between the lowest and highest value of compressive strength was by 44.1 % , P67.5 and P62.5, respectively ($p \leq 0.01$). Additionally, there was no significant difference in compressive modulus of the composites which were found in the range of 0.49-0.93 GPa.

4.4 TGA

Figure 4.4 shows the thermograms of the composites.

The thermograms of composites showed that the weight loss occurred in three main thermal intervals. Initial abrupt weight loss, which is the first interval occurred at approximately 120 °C which is majorly due to loss of absorbed water. In this stage, an additional weight loss might have occurred due to hydrogen bonding deformation between HA and cellulose [59]. The second interval which is between 200 and 500 °C was assigned to thermal degradation of polymeric CMC-Gel composition due to loss of CO_2 of gelatin and decarboxylation of COOH group in CMC [36]. A similar mass loss was also present for the CMC TGA thermogram, which led to 50% weight loss. The third interval which is between 500 and 1200 °C was due to dehydroxylation of HA [2]. In this interval, phase transformation occurred from TTCP-DCPD-CSD to HA with the decomposition of the powder phase [63].

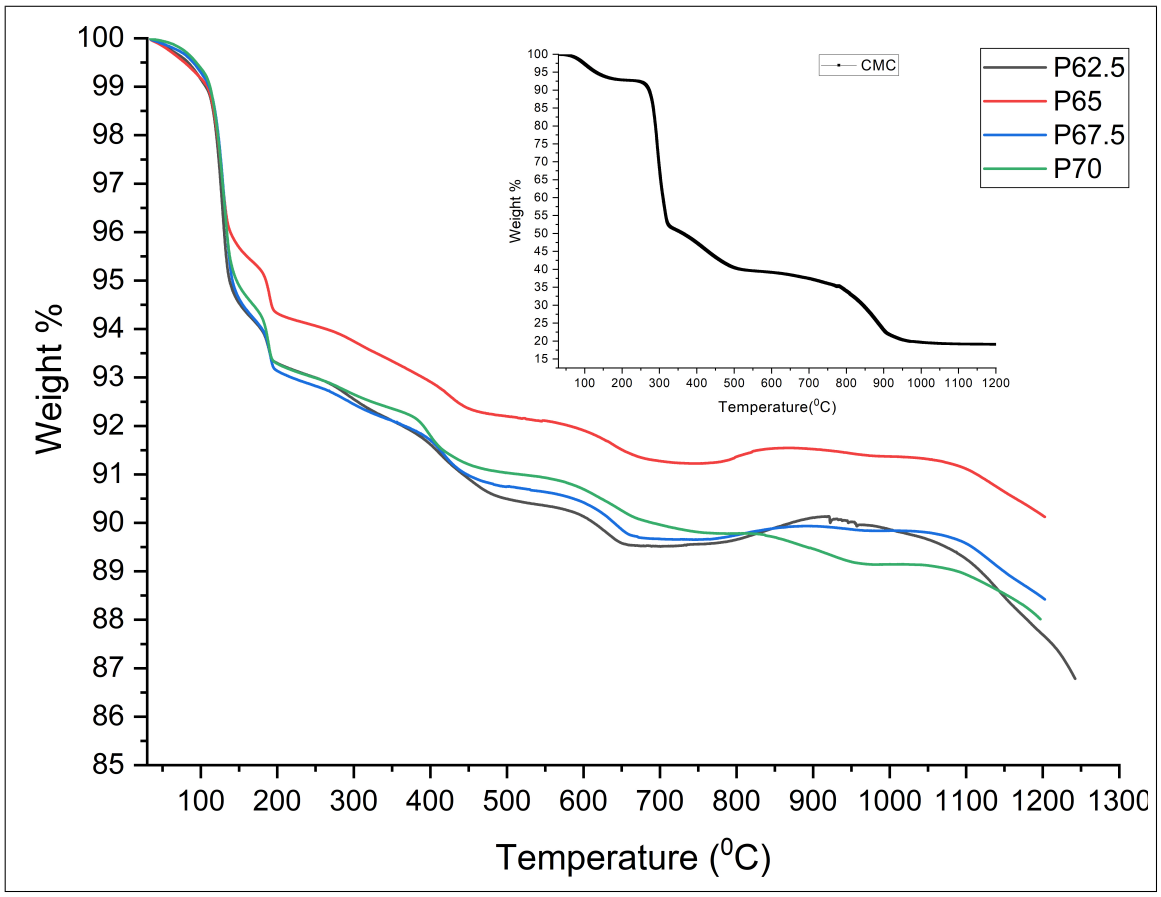

Figure 4.4 TGA thermogram of all composites and CMC.

4.5 XRD

XRD patterns of composites on day 0 and day 28 are shown in Figure 4.5. Peaks at 25.9° and 31.8° on the spectrum represent the main diffraction for HA observing in all composites [36, 57]. Moreover, diffraction peaks which were observed at 29.2° and 20.7° corresponded to characteristic peaks for TTCP and CSD respectively [64, 65].

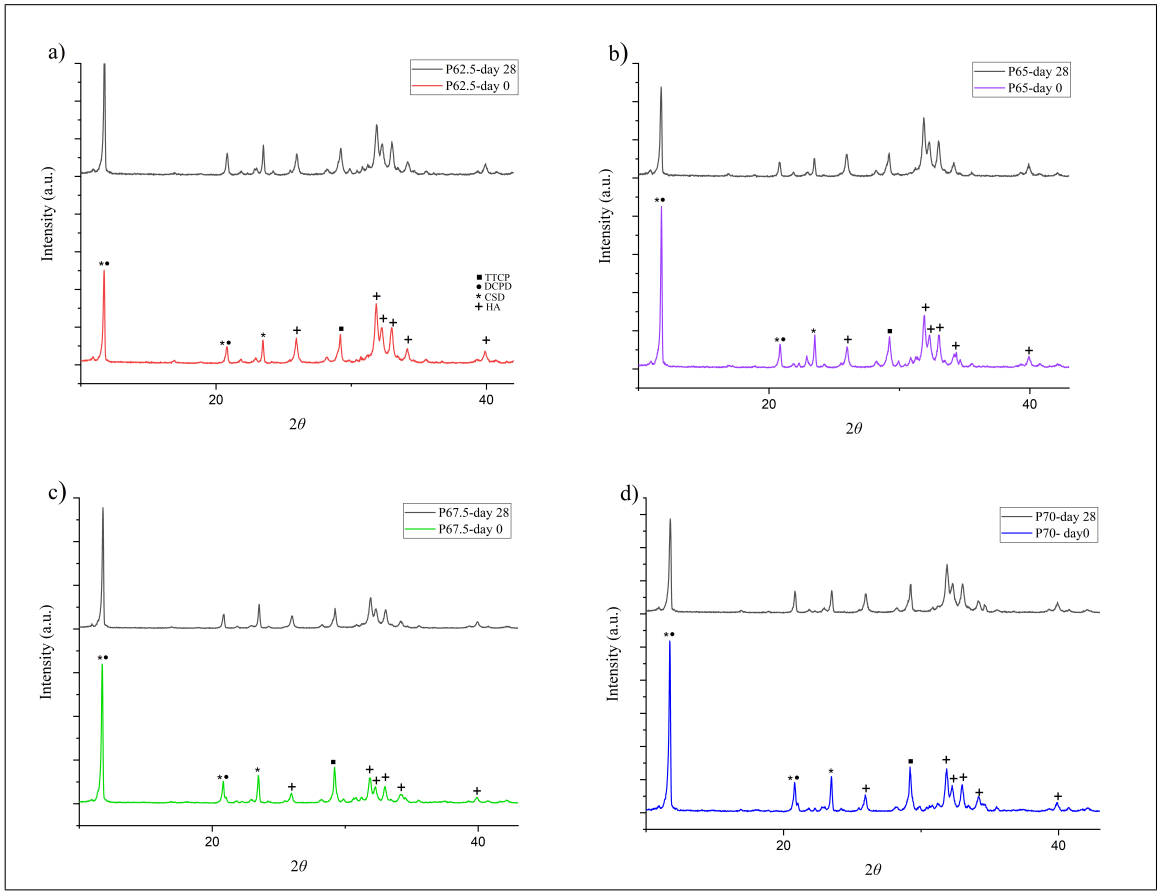

Figure 4.5 XRD patterns of P62.5 (a), P65 (b), P67.5 (c), and P70 (d) for day 0 and day 28.

5. DISCUSSION

In this study, calcium phosphate and calcium sulphate-based powder were incorporated to polymeric hydrogel mainly containing CMC and gelatin to produce novel bone cement. The prediction of interaction and structure of composites during the hardening time were investigated by FTIR. Bands at 3270 and 1627 cm^{-1} were lost when liquid and powder phase were mixed and hardened, which confirmed the electrostatic interaction between negatively charged functional group (COO^- and OH^- molecules) of CMC and positively charged Ca^{2+} ions from CPCs [50]. These bands were also assigned to intramolecular hydrogen bonds and the deformation modes of hydroxyl groups of CMCs, respectively [60]. Furthermore, Qi et al showed that this chelation can promote to perform homogenous CaP nucleation [12].

Then, obtained the structure with Ca^{2+} holds the PO_4^{3-} ions released from calcium phosphate powders, which is resulted in formation of HA [66]. XRD analysis illustrated the presence of HA in composites. HA formation was occurred slowly during the 28 days due to that protonated CMC with Ca^{2+} ions is resistance to swell high amount aqueous solution compared to sodium CMC and there is long-term CaP release [12]. Therefore, TTCP and DCPD particles in final product could also be observed in SEM images at the end of 28 days. Further incubation time may be needed for more HA formation. As shown in SEM images, P65 possibly had a most efficient powder-to-liquid ratio to obtain more HA deposition which has the dispersion of homogeneous CaP on the surface of polymer.

The interaction between inorganic and organic phases and the degree of uniformity of powder and liquid phases have effects on mechanical properties of composites. According to mechanical results, over the 65% powder phase in a composite give rise to deterioration of chemical interaction and mechanical interlocking [67, 68]. The reason of high compressive strength value of composite P70 than composite P67.5 is possibly its higher powder content. Mechanical properties of this new composite materials are

promising in bone tissue engineering, which are accordance with that of trabecular bone. Particularly, they have a potential at the callus where new bone tissue growth at the fracture is formed [36].

Moreover, TGA pattern of composites is similar to pure CMC. The evaluation of the TGA analysis is suggested that composite P65 clearly maintained its stability more than the other composites at the high temperature, which might be resistant to the body environment.

Overall, the CPCs incorporated to polymeric hydrogel were successfully prepared and characterized by FTIR, SEM, XRD, TGA, and mechanical tests. So as to mimic the structure of collagen-HA in the natural bone, new composites prepared including CMC polymer and calcium phosphate may be potential candidate in various bone tissue engineering applications.

6. CONCLUSION AND FUTURE STUDIES

Although many studies focused on physicochemical and biological characteristics of bone materials, mechanical tests were conducted in this study, too. Additionally, based on results and discussion of characterizations on composites, particularly, the mechanical properties are suitable for cancellous bone in terms of compressive modulus. Additionally, the present study allows us to see over 65% powder ratio can be a possible ratio in CPCs, and mixing process for P67.5 and P70 was hard to obtain homogenous hardened composites.

In the future, nanomaterials such as multi-walled carbon nanotube (MWCNT) and graphene oxide (GO) will be studied to improve mechanical properties of prepared CPCs. Furthermore, to be an effective bone substitution, in vitro studies are needed to verify their biocompatibility.

REFERENCES

1. Pasqui, D., P. Torricelli, M. De Cagna, M. Fini, and R. Barbucci, "Carboxymethyl cellulose - Hydroxyapatite hybrid hydrogel as a composite material for bone tissue engineering applications," *Journal of Biomedical Materials Research - Part A*, Vol. 102, no. 5, pp. 1568–1579, 2014.

2. Sarkar, C., P. Kumari, K. Anuvrat, S. K. Sahu, J. Chakraborty, and S. Garai, "Synthesis and characterization of mechanically strong carboxymethyl cellulose-gelatin-hydroxyapatite nanocomposite for load-bearing orthopedic application," *Journal of Materials Science*, Vol. 53, no. 1, pp. 230–246, 2018.

3. Perez, R. A., H. W. Kim, and M. P. Ginebra, "Polymeric additives to enhance the functional properties of calcium phosphate cements," *Journal of Tissue Engineering*, Vol. 3, no. 1, pp. 1–20, 2012.

4. Xu, H. H., P. Wang, L. Wang, C. Bao, Q. Chen, M. D. Weir, L. C. Chow, L. Zhao, X. Zhou, and M. A. Reynolds, "Calcium phosphate cements for bone engineering and their biological properties," *Bone Research*, Vol. 5, no. April, pp. 1–19, 2017.

5. Wang, J. C., C. L. Ko, C. C. Hung, Y. C. Tyan, C. H. Lai, W. C. Chen, and C. K. Wang, "Deriving fast setting properties of tetracalcium phosphate/dicalcium phosphate anhydrous bone cement with nanocrystallites on the reactant surfaces," *Journal of Dentistry*, Vol. 38, no. 2, pp. 158–165, 2010.

6. Thai, V. V., and B. T. Lee, "Fabrication of calcium phosphate-calcium sulfate injectable bone substitute using hydroxy-propyl-methyl-cellulose and citric acid," *Journal of Materials Science: Materials in Medicine*, Vol. 21, no. 6, pp. 1867–1874, 2010.

7. Zhang, J., W. Liu, V. Schnitzler, F. Tancret, and J. M. Bouler, "Calcium phosphate cements for bone substitution: Chemistry, handling and mechanical properties," *Acta Biomaterialia*, Vol. 10, no. 3, pp. 1035–1049, 2014.

8. Liao, H., X. F. Walboomers, W. J. Habraken, Z. Zhang, Y. Li, D. W. Grijpma, A. G. Mikos, J. G. Wolke, and J. A. Jansen, "Injectable calcium phosphate cement with PLGA, gelatin and PTMC microspheres in a rabbit femoral defect," *Acta Biomaterialia*, Vol. 7, no. 4, pp. 1752–1759, 2011.

9. Shi, H., W. Zhang, X. Liu, S. Zeng, T. Yu, and C. Zhou, "Synergistic effects of citric acid - sodium alginate on physicochemical properties of α-tricalcium phosphate bone cement," *Ceramics International*, Vol. 45, no. 2, pp. 2146–2152, 2019.

10. Geffers, M., J. Groll, and U. Gbureck, "Reinforcement strategies for load-bearing calcium phosphate biocements," *Materials*, Vol. 8, no. 5, pp. 2700–2717, 2015.

11. Kucko, N. W., R.-P. Herber, S. C. Leeuwenburgh, and J. A. Jansen, "Calcium Phosphate Bioceramics and Cements," *Principles of Regenerative Medicine*, pp. 591–611, 2018.

12. Qi, P., S. Ohba, Y. Hara, M. Fuke, T. Ogawa, S. Ohta, and T. Ito, "Fabrication of calcium phosphate-loaded carboxymethyl cellulose non-woven sheets for bone regeneration," *Carbohydrate Polymers*, Vol. 189, no. December 2017, pp. 322–330, 2018.

13. Gautam, V., K. P. Singh, and V. L. Yadav, "Preparation and characterization of green-nano-composite material based on polyaniline, multiwalled carbon nano tubes and carboxymethyl cellulose: For electrochemical sensor applications," *Carbohydrate Polymers*, Vol. 189, no. February, pp. 218–228, 2018.

14. Rathna, G. V., D. V. Mohan Rao, and P. R. Chatterji, "Hydrogels of gelatin-sodium carboxymethyl cellulose: Synthesis and swelling kinetics," *Journal of Macromolecular Science - Pure and Applied Chemistry*, Vol. 33, no. 9, pp. 1199–1207, 1996.

15. Bigi, A., B. Bracci, and S. Panzavolta, "Effect of added gelatin on the properties of calcium phosphate cement," *Biomaterials*, Vol. 25, no. 14, pp. 2893–2899, 2004.

16. Feng, Q., K. Wei, S. Lin, Z. Xu, Y. Sun, P. Shi, G. Li, and L. Bian, "Mechanically resilient, injectable, and bioadhesive supramolecular gelatin hydrogels crosslinked by weak host-guest interactions assist cell infiltration and in situ tissue regeneration," *Biomaterials*, Vol. 101, pp. 217–228, 2016.

17. Ghanbarzadeh, B., H. Almasi, and A. A. Entezami, "Improving the barrier and mechanical properties of corn starch-based edible films: Effect of citric acid and carboxymethyl cellulose," *Industrial Crops and Products*, Vol. 33, no. 1, pp. 229–235, 2011.

18. Tenhuisen, K. S., and P. W. Brown, "The effects of citric and acetic acids on the formation of calcium-deficient hydroxyapatite at 38 Â°C," *Journal of Materials Science: Materials in Medicine*, Vol. 5, no. 5, pp. 291–298, 1994.

19. Burguera, E. F., H. H. K. Xu, and M. D. Weir, "Injectable and rapid-setting calcium phosphate bone cement with dicalcium phosphate dihydrate," *Journal of Biomedical Materials Research - Part B Applied Biomaterials*, Vol. 77, no. 1, pp. 126–134, 2006.

20. Tamimi, F., B. Kumarasami, C. Doillon, U. Gbureck, D. L. Nihouannen, E. L. Cabarcos, and J. E. Barralet, "Brushite-collagen composites for bone regeneration," *Acta Biomaterialia*, Vol. 4, no. 5, pp. 1315–1321, 2008.

21. Takagi, S., L. C. Chow, S. Hirayama, and F. C. Eichmiller, "Properties of elastomeric calcium phosphate cement-chitosan composites," *Dental Materials*, Vol. 19, no. 8, pp. 797–804, 2003.

22. Burr, D. B., *Basic and Applied*, Elsevier, 2016.

23. Bose, S., S. Vahabzadeh, and A. Bandyopadhyay, "Bone tissue engineering using 3D printing," *Materials Today*, Vol. 16, no. 12, pp. 496–504, 2013.

24. Doblaré, M., J. M. García, and M. J. Gómez, "Modelling bone tissue fracture and healing: A review," *Engineering Fracture Mechanics*, Vol. 71, no. 13-14, pp. 1809–1840, 2004.

25. Murugan, R., and S. Ramakrishna, "Development of nanocomposites for bone grafting," *Composites Science and Technology*, Vol. 65, no. 15-16 SPEC. ISS., pp. 2385–2406, 2005.

26. Marlow, F., A. S. Khalil, and M. Stempniewicz, "Circular mesostructures: Solids with novel symmetry properties," *Journal of Materials Chemistry*, Vol. 17, no. 21, pp. 2168–2182, 2007.

27. Caeiro, J., P. González, and D. Guede, "Biomechanics and bone (& II): trials in different hierarchical levels of bone and alternative tools for the determination of bone strength," *Revista de Osteoporosis y Metabolismo Mineral*, Vol. 5, no. 2, pp. 99–108, 2013.

28. Rho, J.-Y., L. Kuhn-Spearing, and P. Zioupos, "Mechanical properties and the hierarchical structure of bone," *Medical engineering & physics*, Vol. 20, no. 2, pp. 92–102, 1998.

29. Chew, K. K., K. L. Low, S. H. Sharif Zein, D. S. McPhail, L. C. Gerhardt, J. A. Roether, and A. R. Boccaccini, "Reinforcement of calcium phosphate cement with multi-walled carbon nanotubes and bovine serum albumin for injectable bone substitute applications," *Journal of the Mechanical Behavior of Biomedical Materials*, Vol. 4, no. 3, pp. 331–339, 2011.

30. Beer Jr, F. P., "E. russell johnston, john t. dewolf, and david f. mazurek," *Mechanics of Materials. McGraw-Hill, New York*, 2011.

31. Bankoff, A. D. P., "Biomechanical characteristics of the bone," in *Human musculoskeletal biomechanics*, IntechOpen, 2012.

32. Grosfeld, E. C., J. W. M. Hoekstra, R. P. Herber, D. J. Ulrich, J. A. Jansen, and J. J. Van Den Beucken, "Long-term biological performance of injectable and degradable calcium phosphate cement," *Biomedical Materials (Bristol)*, Vol. 12, no. 1, 2017.

33. Bundela, H., and A. K. Bajpai, "Designing of hydroxyapatite-gelatin based porous matrix as bone substitute: Correlation with biocompatibility aspects," *Express Polymer Letters*, Vol. 2, no. 3, pp. 201–213, 2008.

34. Kao, S. T., and D. D. Scott, "A Review of Bone Substitutes," *Oral and Maxillofacial Surgery Clinics of North America*, Vol. 19, no. 4, pp. 513–521, 2007.

35. Laurencin, C., Y. Khan, and S. F. El-Amin, "Bone graft substitutes," *Expert Review of Medical Devices*, Vol. 3, no. 1, pp. 49–57, 2006.

36. Manjubala, I., P. Basu, and U. Narendrakumar, "In situ synthesis of hydroxyapatite/carboxymethyl cellulose composites for bone regeneration applications," *Colloid and Polymer Science*, pp. 1729–1737, 2018.

37. Pooput, K., N. Monmaturapoj, J. Sansatsadeekul, S. Channasanon, and A. Srion, "Preparation and characterization of calcium phosphate bone cement with rapidly-generated tubular macroporous structure by incorporation of polysaccharide-based microstrips," *Ceramics International*, Vol. 43, no. 4, pp. 3616–3622, 2017.

38. An, J., J. G. Wolke, J. A. Jansen, and S. C. Leeuwenburgh, "Influence of polymeric additives on the cohesion and mechanical properties of calcium phosphate cements," *Journal of Materials Science: Materials in Medicine*, Vol. 27, no. 3, pp. 1–9, 2016.

39. Sugawara, A., K. Asaoka, and S. J. Ding, "Calcium phosphate-based cements: Clinical needs and recent progress," *Journal of Materials Chemistry B*, Vol. 1, no. 8, pp. 1081–1089, 2013.

40. Dorozhkin, S., "Self-Setting Calcium Orthophosphate Formulations," *Journal of Functional Biomaterials*, Vol. 4, no. 4, pp. 209–311, 2013.

41. Elahpour, N., S. M. Rabiee, M. H. Ebrahimzadeh, and A. Moradi, "In-vitro formation and growth kinetics of apatite on a new light-cured composite calcium phosphate cement," *Ceramics International*, Vol. 44, no. 13, pp. 15317–15322, 2018.

42. Oğuz, Ö. D., and D. Ege, "Rheological and mechanical properties of thermoresponsive methylcellulose/calcium phosphate-based injectable bone substitutes," *Materials*, Vol. 11, no. 4, 2018.

43. Yokoyama, A., S. Yamamoto, T. Kawasaki, T. Kohgo, and M. Nakasu, "Development of calcium phosphate cement using chitosan and citric acid for bone substitute materials," *Biomaterials*, Vol. 23, no. 4, pp. 1091–1101, 2002.

44. Nilsson, M., E. Fernández, S. Sarda, L. Lidgren, and J. A. Planell, "Characterization of a novel calcium phosphate/sulphate bone cement," *Journal of Biomedical Materials Research*, Vol. 61, no. 4, pp. 600–607, 2002.

45. Gao, C., S. Huo, X. Li, X. You, Y. Zhang, and J. Gao, "Characteristics of calcium sulfate/gelatin composite biomaterials for bone repair," *Journal of Biomaterials Science, Polymer Edition*, Vol. 18, no. 7, pp. 799–824, 2007.

46. Bohner, M., "New hydraulic cements based on α-tricalcium phosphate-calcium sulfate dihydrate mixtures," *Biomaterials*, Vol. 25, no. 4, pp. 741–749, 2004.

47. Varma, D. M., G. T. Gold, P. J. Taub, and S. B. Nicoll, "Injectable carboxymethylcellulose hydrogels for soft tissue filler applications," *Acta Biomaterialia*, Vol. 10, no. 12, pp. 4996–5004, 2014.

48. Aravamudhan, A., D. M. Ramos, A. A. Nada, and S. G. Kumbar, "Natural polymers: polysaccharides and their derivatives for biomedical applications," in *Natural and synthetic biomedical polymers*, pp. 67–89, Elsevier, 2014.

49. Agis, H., B. Beirer, G. Watzek, and R. Gruber, "Effects of carboxymethylcellulose and hydroxypropylmethylcellulose on the differentiation and activity of osteoclasts and osteoblasts," *Journal of Biomedical Materials Research - Part A*, Vol. 95 A, no. 2, pp. 504–509, 2010.

50. Varela Caselis, J., E. Reyes Cervantes, G. Landeta Cortés, R. Agustín Serrano, and E. Rubio Rosas, "Hydroxyapatite growth on cotton fibers modified chemically," *Materials Science-Poland*, Vol. 32, no. 3, pp. 436–441, 2014.

51. Rokhade, A. P., S. A. Agnihotri, S. A. Patil, N. N. Mallikarjuna, P. V. Kulkarni, and T. M. Aminabhavi, "Semi-interpenetrating polymer network microspheres of gelatin and sodium carboxymethyl cellulose for controlled release of ketorolac tromethamine," *Carbohydrate Polymers*, Vol. 65, no. 3, pp. 243–252, 2006.

52. Dickens, F., "The citric acid content of animal tissues, with reference to its occurrence in bone and tumour.," *The Biochemical journal*, Vol. 35, no. 8-9, pp. 1011–23, 1941.

53. Khalyfa, A., S. Vogt, J. Weisser, G. Grimm, A. Rechtenbach, W. Meyer, and M. Schnabelrauch, "Development of a new calcium phosphate powder-binder system for the 3D printing of patient specific implants," *Journal of Materials Science: Materials in Medicine*, Vol. 18, no. 5, pp. 909–916, 2007.

54. Song, H. Y., A. H. Esfakur Rahman, and B. T. Lee, "Fabrication of calcium phosphate-calcium sulfate injectable bone substitute using chitosan and citric acid," *Journal of Materials Science: Materials in Medicine*, Vol. 20, no. 4, pp. 935–941, 2009.

55. Demitri, C., R. Del Sole, F. Scalera, A. Sannino, G. Vasapollo, A. Maffezzoli, L. Ambrosio, and L. Nicolais, "Novel superabsorbent cellulose-based hydrogels crosslinked with citric acid," *Journal of Applied Polymer Science*, Vol. 110, no. 4, pp. 2453–2460, 2008.

56. Saputra, A. H., M. Hapsari, A. B. Pitaloka, and P. Wulan, "Synthesis and characterization of hydrogel from cellulose derivatives of water hyacinth (Eichhornia crassipes) through chemical cross-linking method by using citric acid," *Journal of Engineering Science and Technology*, Vol. 10, no. October, pp. 75–86, 2015.

57. Jayasree, R., T. S. Sampath Kumar, R. P. Nankar, and M. Doble, "Accelerated Self-Hardening Tetracalcium Phosphate Based Bone Cement with Enhanced Strength and Biological Behaviour," *Transactions of the Indian Institute of Metals*, Vol. 68, no. 2, pp. 299–304, 2015.

58. Song, Y., Z. Feng, and T. Wang, "In situ study on the curing process of calcium phosphate bone cement," *Journal of Materials Science: Materials in Medicine*, Vol. 18, no. 6, pp. 1185–1193, 2007.

59. Garai, S., and A. Sinha, "Biomimetic nanocomposites of carboxymethyl cellulose-hydroxyapatite: Novel three dimensional load bearing bone grafts," *Colloids and Surfaces B: Biointerfaces*, Vol. 115, pp. 182–190, 2014.

60. Duhoranimana, E., E. Karangwa, L. Lai, X. Xu, J. Yu, S. Xia, X. Zhang, B. Muhoza, and I. Habinshuti, "Effect of sodium carboxymethyl cellulose on complex coacervates formation with gelatin: Coacervates characterization, stabilization and formation mechanism," *Food Hydrocolloids*, Vol. 69, pp. 111–120, 2017.

61. Medvecky, L., M. Giretova, and T. Sopcak, "Preparation and properties of tetracalcium phosphate-monetite biocement," *Materials Letters*, Vol. 100, pp. 137–140, 2013.

62. Burguera, E. F., F. Guitián, and L. C. Chow, "A water setting tetracalcium phosphate-dicalcium phosphate dihydrate cement," *Journal of Biomedical Materials Research - Part A*, Vol. 71, no. 2, pp. 275–282, 2004.

63. Duarte, E. B., B. S. das Chagas, F. K. Andrade, A. I. Brígida, M. F. Borges, C. R. Muniz, M. d. S. M. Souza Filho, J. P. Morais, J. P. Feitosa, and M. F. Rosa, "Production of hydroxyapatite-bacterial cellulose nanocomposites from agroindustrial wastes," *Cellulose*, Vol. 22, no. 5, pp. 3177–3187, 2015.

64. Ding, Y., S. Tang, B. Yu, Y. Yan, H. Li, J. Wei, and J. Su, "In vitro degradability, bioactivity and primary cell responses to bone cements containing mesoporous magnesium-calcium silicate and calcium sulfate for bone regeneration," *Journal of the Royal Society Interface*, Vol. 12, no. 111, 2015.

65. Fukase, Y., E. D. Eanes, S. Takagp, L. C. Chow, and W. E. Brown, "Setting Reactions and Compressive Strengths of Calcium Phosphate Cements," *Journal of Dental Research*, Vol. 69, no. 12, pp. 1852–1856, 1990.

66. Kumar, B., and Y. S. Negi, "Water absorption and viscosity behaviour of thermally stable novel graft copolymer of carboxymethyl cellulose and poly(sodium 1-hydroxy acrylate)," *Carbohydrate Polymers*, Vol. 181, no. July 2017, pp. 862–870, 2018.

67. Jiang, L. Y., Y. B. Li, L. Zhang, and X. J. Wang, "Preparation and characterization of a novel composite containing carboxymethyl cellulose used for bone repair," *Materials Science and Engineering C*, Vol. 29, no. 1, pp. 193–198, 2009.

68. Liuyun, J., L. Yubao, Z. Li, and L. Jianguo, "Preparation and properties of a novel bone repair composite: Nano-hydroxyapatite/chitosan/carboxymethyl cellulose," *Journal of Materials Science: Materials in Medicine*, Vol. 19, no. 3, pp. 981–987, 2008.